

REAL-TIME EMPIRICAL MODE DECOMPOSITION FOR EEG SIGNAL ENHANCEMENT

Alina Santillán-Guzmán, Martin Fischer, Ulrich Heute, Gerhard Schmidt

Kiel University, Faculty of Engineering
Digital Signal Processing and System Theory
24143 Kiel, Germany

ABSTRACT

Electroencephalography (EEG) recordings are used for brain research. However, in most cases, the recordings not only contain brain waves, but also artifacts of physiological or technical origins. A recent approach used for signal enhancement is Empirical Mode Decomposition (EMD), an adaptive data-driven technique which decomposes non-stationary data into so-called Intrinsic Mode Functions (IMFs). Once the IMFs are obtained, they can be used for denoising and detrending purposes. This paper presents a real-time implementation of an EMD-based signal enhancement scheme. The proposed implementation is used for removing noise, for suppressing muscle artifacts, and for detrending EEG signals in an automatic manner and in real-time. The proposed algorithm is demonstrated by application to a simulated and a real EEG data set from an epilepsy patient. Moreover, by visual inspection and in a quantitative manner, it is shown that after the EMD in real-time, the EEG signals are enhanced.

Index Terms— EMD, real-time, denoising, detrending, EEG

1. INTRODUCTION

In neurological research, the recording and analysis of electrical fields from the brain play an important role. The technique used to measure these electrical fields is called Electroencephalography (EEG) [1]. The recorded EEG data are often distorted by other signals, called artifacts, whose origins are either of physiological or technical nature. There have been proposed many techniques to identify, separate, and suppress these artifacts from the EEG signals. One of the most common techniques used for that purpose is Independent Component Analysis (ICA) [2]. However, ICA does not work well for highly non-stationary artifacts such as muscle artifacts.

In 1998, Norden E. Huang et al. proposed a new method for analyzing non-stationary data [3]. This technique is known as the Huang-Hilbert transform (HHT). The HHT uses a novel preprocessing algorithm, the Empirical Mode

Decomposition (EMD), to decompose an arbitrary signal into a sum of so-called Intrinsic Mode Functions (IMFs) and a residue. Based on the inherent characteristics of the IMFs, the EMD can be used for denoising and detrending purposes.

In order to denoise the signals, it has been suggested in [4] to remove the IMFs that are considered to be dominated by noise. The supervision of an expert is required to determine which IMFs can be removed without losing physiological information. Other methods are based on thresholds which are computed from statistical properties of the signals. However, most of these properties can only be determined after recording the data [5]. In [6], a hardware architecture for computing the EMD on-line has been proposed. An interpolation method with data reuse was applied in order to reduce time delays and memory usage. This was the first attempt to implement the HHT on-line and on-chip.

The main objective of this paper is to present the EMD algorithm in real-time as a software implementation. The proposed algorithm has been applied to real EEG signals contaminated with simulated muscle artifacts, and real EEG signals from an epilepsy patient with inherent muscle artifacts. The purpose of this application is to detrend the signals, remove noise and suppress muscle artifacts that are contaminating the physiological information. In section 2, the algorithm is described. The quantitative measure used to compare the signals before and after the application of the EMD in real-time is described in section 3. Section 4 contains the results of both data sets. Conclusions are given in section 5.

2. EMPIRICAL MODE DECOMPOSITION IN REAL-TIME

The EMD [3, 7] decomposes an arbitrary input signal $x(t)$ into a set of N IMFs ($IMF_i(t)$) plus a residue ($r_N(t)$), which can be either a constant, a trend, or a curve having only one extremum. The real-time implementation of the EMD requires a block-wise processing structure. Therefore, a few changes have been applied to the offline EMD algorithm proposed in [3, 8]. For the real-time case, the input signal could be expressed as:

$$x_k(t) = \sum_{i=1}^N IMF_{i,k}(t) + r_{N,k}(t), \quad (1)$$

This work was supported by the German Research Foundation (Deutsche Forschungsgemeinschaft, DFG) through the Collaborative Research Center SFB 855 "Biomagnetic Sensing"

where k corresponds to the k -th block. An IMF is any function that fulfills two conditions: *i*) The numbers of extrema and zero crossings are equal or differ at most by one; *ii*) the mean value between the upper and lower envelopes, defined by all local maxima and minima, is zero at any point. The procedure to identify and extract single IMFs from a given data set is called sifting process.

For the real-time EMD, the input signals are passed to buffers of a certain length. According to [9], for EEG signals, a buffer size of at least 0.5 seconds is enough to force slowly varying trends into higher IMFs. However, it has been observed that larger buffer sizes still lead to satisfactory results. This amount of data will cause a heavy workload because the EMD is applied to many input channels at once. Moreover, as stated above, the processing is carried out block-wise. For those reasons, the EMD is computed in an extra thread to guarantee real-time processing.

As in the offline case, the real-time EMD procedure begins with localization of all extrema of each input signal block. The local maxima are used to determine the upper envelope, $u_k(t)$, while all local minima are used to determine the lower envelope, $l_k(t)$. Both, maxima and minima, are found by means of cubic spline interpolation, which is the key part of the EMD algorithm. In this work, it has been computed according to [10]. The implementation is based on the fact that the equations for the spline interpolation can be solved using a tridiagonal matrix algorithm.

A problem that may arise, comes from the boundary conditions for the cubic spline interpolation, which might introduce errors at the boundary intervals of the envelopes [6]. To solve this problem, the first and last samples are considered as extrema for both, the upper and lower envelopes. The boundary error is further reduced by overlapping subsequent results of the EMD process and by applying a Hann-window to the output of the EMD. An overlap of 50% has been chosen in this work. To keep the number of output samples constant, the buffer size for the EMD is twice the length of the input buffer. Due to the windowing, the EMD results from the previous and the next processing steps are required to achieve a complete output.

The next step consists of computing the mean curve, $m_{1,k}(t)$, of the upper and lower envelope at each time instant. Then, by taking the difference between the data and the computed mean, a first *proto-IMF* ($pIMF_{1,k}(t)$) is obtained:

$$pIMF_{1,k}(t) = x_k(t) - m_{1,k}(t). \quad (2)$$

In the next step, $pIMF_{1,k}(t)$ is assumed to be the new input data to the process, and all of the above steps are repeated again.

In the offline EMD, the sifting process is terminated when any of two stoppage criteria are fulfilled [3]. The first one tests the relative discrepancy between two consecutive sifting steps. It is called sum of differences (SD). It has to be smaller than a preassigned threshold. The second stoppage criterion

is based on the definition of an IMF and is used to guarantee a stable range for SD. It checks the number of consecutive siftings, when the numbers of zero-crossings and extrema are equal or differ at most by one. It is called the S-number and its value depends on the data that is being processed. In the real-time EMD, these two criteria are not longer valid. Instead, a fixed number of iterations for the sifting process is used to ensure comparability of the IMFs for consecutive blocks.

After M iterations (where M is the fixed value for the amount of sifting-process iterations), the first IMF of every block k , $IMF_{1,k}(t)$, can be found and it can be separated from the rest of the data according to:

$$r_{1,k}(t) = x_k(t) - IMF_{1,k}(t). \quad (3)$$

The remaining signal is treated as the new input for the sifting process. The whole procedure will stop after N IMFs have been extracted (where N is a value predefined by the user, depending on the application) or whenever the number of extrema is smaller than two. The last IMF is considered as the residue, which is assumed to be a constant, a monotonic slope, or a curve having only one extremum.

After the IMFs and residue have been obtained, the enhancement of the signals takes place.

2.1. Denoising

As stated above, several methods have been proposed to remove the noise and preserve the physiological information using EMD. However, the supervision of an expert is needed in order to determine which IMFs can be removed without losing information. In order to do it in an automatic manner and in real-time, we have assumed that the physiological signals lie in a frequency band from 0 Hz to a specific cut-off frequency. All frequency components that are above this limit are attenuated. For that purpose, a measure similar to the signal-to-noise ratio has been introduced. It is computed for every block and each IMF, assuming that most of the undesired components lie in the high frequency range. This ratio is defined as:

$$R(i, k) = 10 \cdot \log_{10} \left(\frac{P_{signal}(i, k)}{P_{noise}(i, k)} \right) [dB], \quad (4)$$

where $P_{signal}(i, k)$ denotes the signal power, i.e., the sum of the power of all frequency bins up to the cut-off frequency of the i -th IMF and the k -th block, whereas $P_{noise}(i, k)$ is the power of the noise calculated from the sum of the powers of the frequency bins above the frequency limit. Both powers are calculated by applying FFTs to the IMFs. Afterwards, the power spectral density is computed for each IMF and for the residue.

An IMF is assumed to be dominated by noise, when its R value is below a predefined threshold TH_{noise} . A denoising factor is then multiplied to the noisy modes to attenuate the

noise. The denoising factor is computed by

$$a_{den}(i,k) = \begin{cases} 1, & \text{if } R_{i,k} \geq TH_{noise}, \\ 10^{\frac{R_{i,k} - TH_{noise}}{10}}, & \text{else.} \end{cases} \quad (5)$$

In this work, the cut-off frequency has been set to 30 Hz, and $TH_{noise} = 0$ dB.

Due to the frequency limit, the signals are not only denoised, but also the muscle (as well as other) artifacts that lie above the cutoff frequency are suppressed.

2.2. Detrending

The method proposed by [11], which uses the amount of energy to identify the boundary between noise and signal components, has been used in this work in order to detrend the data. The energy of each IMF, $E_{i,k}$, has been calculated according to [11]:

$$E_{i,k} = \sum_{t=1}^T IMF_{i,k}^2(t), \quad (6)$$

where T is the number of samples per block. In the offline processing, the point when the energy of the first IMFs reaches its lowest value is considered as a boundary between the noise and signal components. For the real-time processing, it is not possible to derive a reliable boundary because the energy levels in the IMFs vary from one block to the other. However, a comparison of the energy levels in the residue with the local trends has shown a direct proportional relationship. Therefore, this association can be used for detrending purposes, assuming that the trend is forced into the residue due to the block-wise processing. According to [12], the energy of the original signal, $E_{o,k}$, is equal to the sum of energies of the IMFs plus the energy of the residue. Mathematically, this is given by

$$E_{o,k} = \sum_{i=1}^N E_{i,k} + Er_k, \quad (7)$$

where Er_k is the energy of the residual and $E_{i,k}$ is the energy of the i -th IMF of block k . A parameter to describe the energy relations among the IMFs and the residue has been introduced, namely the energy coefficient $\eta_{i,k}$:

$$\eta_{i,k} = \frac{E_{i,k}}{E_{o,k}} \quad \text{and} \quad \eta_{r_k} = \frac{Er_k}{E_{o,k}}. \quad (8)$$

Since the energy coefficient is normalized by $E_{o,k}$, $\eta_{i,k}$ is in the range from zero to one. The energy coefficient is used to attenuate the IMF that represents the local trend, usually the residue. This attenuation is carried out by computing a factor that is multiplied with the IMF that has to be attenuated. Therefore, the multiplication factor is determined by

$$a_{detrend}(k) = 1 - \eta_{r_k} \quad (9)$$

The more the residual is differing from zero, the higher is its energy coefficient η_{r_k} and the stronger is its attenuation. The multiplication factor will be one, if the signal has zero mean. The energy coefficient computation, as well as the attenuation is performed block-wise, as stated above.

3. QUANTITATIVE MEASURE

The results of the EMD are compared not only by visual inspection, but also by a quantitative measure. The variances of an artifacts-free segment (σ_{Sig1}^2) and a segment with artifacts (σ_{Sig2}^2), before and after the EMD, have been computed as a measure of signal enhancement. It is expected that after the EMD the variance of the filtered artifactual segment is very similar to the variance of the artifacts-free segment. The following ratio VR is then computed:

$$VR(l) = \frac{mean_p(\sigma_{Sig1}^2(l,p))}{mean_p(\sigma_{Sig2}^2(l,p))}, \quad (10)$$

where l denotes the channel number and p the block number; $mean_p$ corresponds to the arithmetic mean over all blocks. The length of each block to compute the variance is equal to 0.5 s. The closer to one this ratio is, the more similar the variances are, indicating that the signals have been enhanced.

4. RESULTS

The EMD algorithm in real-time as described above was applied to a semi-simulated data set and to a real EEG data set from an epilepsy patient. In the following, the results are explained.

4.1. Study on semi-simulated data

In order to test the performance of the EMD in real-time, semi-simulated EEG data were created: Real EEG signals from the central and frontal parts of the brain were contaminated with simulated muscle artifacts. The length of the signals was 60 s. The sampling frequency of the original signals was equal to 5 kHz. However, the sampling frequency of the platform that has been used is 44.1 kHz; for this reason, the data were upsampled to that frequency in order to use them as input signals for the platform. Then, they were internally downsampled to 1378 Hz = 44.1 kHz/32 before processing.

To simulate the contaminated signals, a real muscle artifact was taken from real EEG epilepsy data by band-pass filtering (from 30-300 Hz). The obtained muscle artifact was added to real artifacts-free EEG signals in intervals where spikes are present. An example of a contaminated signal is shown in Fig.1a (dotted-line).

The contaminated signals were passed through the EMD in real-time. The length of each input block to be processed was equal to 2 s. It is mentioned in [11] that at least 10 iterations are necessary to guarantee stability and convergence

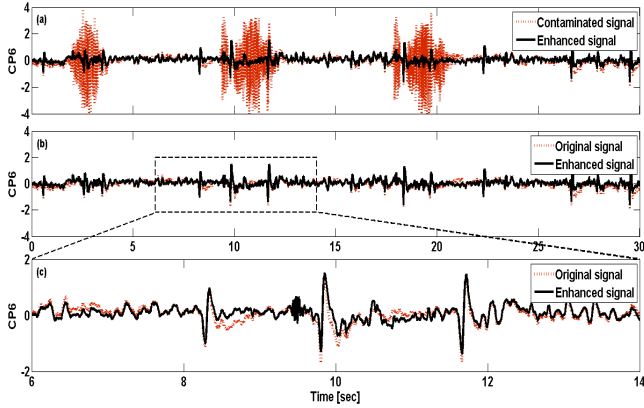


Fig. 1. (a) Semi-simulated EEG signal of electrode CP6 contaminated with muscle artifacts before (dotted-line) and after (continuous line) EMD; (b) Original signal before contamination with muscle artifacts (dotted-line) and after the application of the EMD (continuous line); (c) Zoom-in of the same signals before contamination (dotted-line) and after EMD (continuous line).

of the IMFs. Therefore, the number of sifting iterations and the total number of IMFs to be computed were set to 12. The muscle artifacts were assumed to be above 30 Hz; therefore, the cutoff frequency to compute the denoising factor was set to 30 Hz. For detrending, the detrending factor was computed and multiplied with the last IMF, i.e., the residue.

The enhanced signal is shown in Fig.1a (continuous line). As can be observed, after enhancing the signals, the spikes are visible and the muscle artifacts are suppressed.

Figure 1b shows the original signal before adding the muscle artifacts (dotted-line), and the signal after the application to EMD (continuous line). As expected, after the EMD, these signals are very similar. In order to better observe this similarity, Fig. 1c shows a close-up of part of the signal plotted in Fig. 1b. It can be observed in this figure that the signal after EMD has been denoised and detrended.

Table 1 presents the results of the parameter VR of five EEG signals, before (VR_O) and after (VR_{EMD}) the application of EMD. The first two rows correspond to semi-simulated signals. The first column contains the electrode labels, which are standard according to the 10-20 International EEG system. As expected, after EMD, VR_{EMD} is close to one. That is an indication that the enhanced signal is very similar to the original signal before adding the muscle artifacts.

In one of the cases (signal CP6) the result is slightly above one. That suggests that after EMD some loss of information has occurred. However, the suppression of the muscle artifacts and the detrending of the signals was qualitatively acceptable.

4.2. Results with Real Data

A real EEG data set from an epilepsy patient was also employed. A total of 30 EEG channels of 60 s length have been

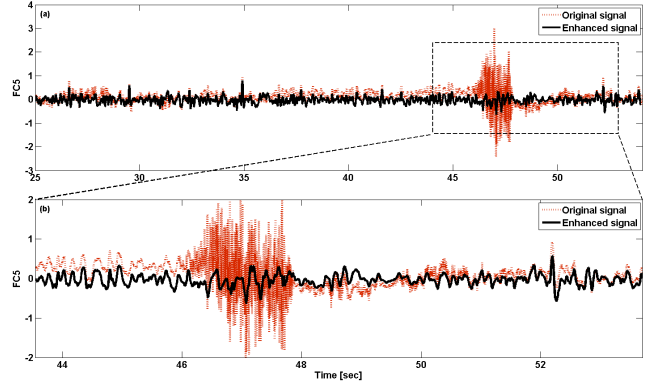


Fig. 2. (a) EEG signal of electrode FC5 contaminated with muscle artifacts before (dotted-line) and after (continuous line) EMD. (b) Zoom-in of the same signal before (dotted-line) and after (continuous line) EMD.

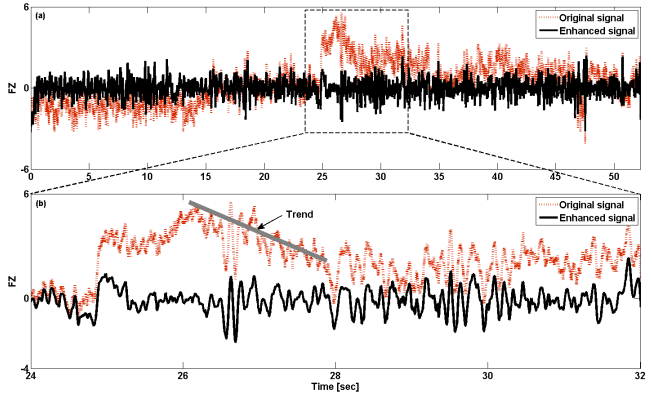


Fig. 3. (a) EEG signal of electrode FZ presenting a trend behavior before (dotted-line) and after (continuous line) EMD. (b) Zoom-in of the same signal before (dotted-line) and after (continuous line) EMD. The trend is pointed out with an arrow and a diagonal line.

enhanced at once. The same settings as for the semi-simulated case were used for the real case.

Figure 2a shows the contaminated data (dotted-line) corresponding to signal FC5. As can be observed, the signal is contaminated with muscle artifacts in the last 15 s. On the same figure, the enhanced signal (continuous line) is plotted. It can be observed in the figure that the spikes are still preserved and the muscle artifact has been suppressed. Figure 2b shows a zoom-in of the artifactual region. In this figure, it can be seen, by looking carefully, that the signal has been detrended and that the physiological waves are still present.

In Fig. 3, an example where detrending is better observed is presented. As shown in Fig. 3a, a signal having a strong trend is presented before (dotted-line) and after (continuous line) the application of the EMD. In Fig. 3b, a zoom-in of the trend region is plotted. As can be seen in the figure, the trend has been reduced. Moreover, the noise contained in the original signal has been suppressed, and the physiological information is still preserved.

Table 1. Quantitative measure of signal enhancement before (VR_O), and after (VR_{EMD}) EMD.

Electrode	VR_O	VR_{EMD}
CP6	0.19	1.02
FP1	0.12	0.98
FC5	0.22	0.97
FZ	0.62	0.87
C4	0.65	0.83

In the last three rows of Table 1 the parameter VR of three real EEG signals is presented, including the signals shown in Figs. 2 and 3.

Again, it is expected that the ratio after EMD is close to one. According to this, it can be seen that in all cases, the signals have been enhanced in comparison with the original: The muscle artifacts and noise are reduced and the trend has also been removed.

5. CONCLUSION

In this paper, the use of an EMD in real-time for the enhancement of EEG signals has been introduced. The noise, the muscle artifacts, and the trend of the signals were successfully removed. This has been achieved in an automatic manner by computing denoising and detrending factors which were multiplied with the IMFs considered as noise-dominated or trend-dominated.

The entire system was implemented on a standard PC and 30 EEG channels could be easily processed at a sample rate of $44.1 \text{ kHz}/32 = 1378 \text{ Hz}$.

Two cases were analyzed, namely, a semi-simulated EEG data set and a real EEG data set from an epilepsy patient. In both cases, the signals have been enhanced: The trends have been removed, the noise, and the muscle artifacts have been suppressed. As a reference for the semi-simulated case, the signals before being contaminated with muscle artifacts were used. According to the results, after EMD the reference and the enhanced signal are very similar, indicating that the muscle artifacts were successfully suppressed.

The ratio VR has been used as a measure of signal enhancement. It has taken into account the variance of the artifacts-free segment and the segment with artifacts before and after the application to EMD. According to the results, the signals after EMD have been enhanced, in comparison with the original signals.

Further research will focus on the control mechanism to denoise and detrend the signals. This has to be done in order to avoid any loss of physiological information. Moreover, a comparison with other filtering techniques should be performed. Another topic that should be addressed in the future is the mode-mixing, i.e., when the separation is not good enough because the signals have similar frequencies.

6. REFERENCES

- [1] S. Sanei and J.A Chambers, *EEG Signal Processing*, John Wiley & Sons, 2007.
- [2] A. Hyvärinen and E. Oja, "Independent Component Analysis: Algorithms and Applications," *Neural Networks*, vol. 13, pp. 411 – 430, 2000.
- [3] N.E. Huang, Z. Shen, S.R. Long, M.L. Wu, H.H. Shih, Q. Zheng, N.C. Yen, C.C. Tung, and H.H. Liu, "The Empirical Mode Decomposition and Hilbert Spectrum for Nonlinear and Non-stationary Time Series Analysis," *Proc. Roy. Soc.*, vol. 454, pp. 903 – 995, 1998.
- [4] Z. De-xiang, W. Xiao-pei, and G. Xiao-jing, "The EEG Signal Preprocessing Based on Empirical Mode Decomposition," in *Proc. 2nd Int. Conf. on Bioinformatics and Biomedical Engineering (ICBBE)*, 2008.
- [5] H. Nolan, R. Whelan, and R.B. Reilly, "FASTER: Fully Automated Statistical Thresholding for EEG Artifact Rejection," *Journal of Neuroscience Methods*, vol. 192, pp. 152 – 162, 2010.
- [6] N.-F. Chang, C. Cheng-Yi, T.-C. Chen, and L.-G. Chen, "On-line Empirical Mode Decomposition Biomedical Microprocessor for Hilbert Huang Transform," in *Proc. Conf. on Biomedical Circuits and Systems Conference (BioCAS)*, IEEE, pp. 420 – 423, 2011.
- [7] N.E. Huang and N.O. Attoh-Okine, *The Hilbert-Huang Transform in Engineering*, CRC Press, June 2005.
- [8] G. Rilling, P. Flandrin, and P. Goncalves, "On Empirical Mode Decomposition and its Algorithms," in *Proc. 6th IEEE-EURASIP Workshop on Nonlinear Signal and Image Processing (NSIP)*, 2003.
- [9] B.S. Raghavendra and D. Narayana Dutt, "Correction of Ocular Artifacts in EEG Recordings using Empirical Mode Decomposition," *National Conference on Communication*, pp. 327 – 330, 2007.
- [10] W.H. Press, S.A. Teukolsky, W.T. Vetterling, and B.P. Flannery, *Numerical Recipes In C: The Art of Scientific Computing*, Cambridge University Press, 1992.
- [11] N.E. Huang and Z. Wu, "A study of the characteristics of white noise using the empirical mode decomposition method," *Proc. Roy. Soc.*, vol. 460, pp. 1597 – 1611, 2004.
- [12] D. Yang, C. Rehtanz, Y. Li, Q. Liu, and K. Görner, "Denoising and Detrending of Measured Oscillatory Signal in Power System," *Electrical Review*, vol. 88, pp. 135 – 139, 2012.